Supporting information

Selective electrosynthesis of aldehydes at industrially relevant current densities via tandem electrochemical-chemical catalysis

Ting Lin，Menglu Cai, Huijie Chen and Yiming Mo*

College of Chemical and Biological Engineering, Zhejiang University, Hangzhou, 310027, Zhejiang, China; ZJU-Hangzhou Global Scientific and Technological Innovation Center, Zhejiang University, Hangzhou, 311215, China.

Email: yimingmo@zju.edu.cn.

1. Reagents and materials

All the fluidic connections and PTFE tubes were from IDEX (https://www.idex-hs.com/) and Runze Fluid (https://www.runzefluidsystem.com/). All stainless-steel ferrule fittings were from Xiongchuan. All commercially available chemical reagents and solvents were used directly without further purification.
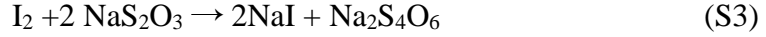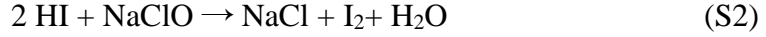
2. Characterization

Gas chromatography analysis was conducted on Agilent 8890 GC system with an FID detector. High-performance liquid chromatography analysis was conducted on Agilent 1260 Infinity II HPLC system.

3. Determination of hypochlorite concentration

The concentration of hypochlorite in the solution generated was initially roughly determined using an ultraviolet-visible spectrophotometer (X8 from Shanghai Yuan Analysis). The exact concentration of hypochlorite was measured using the iodometric method. 2.0 mL of solution was withdrawn from the sample solution containing electrochemically generated hypochlorite, excess KI was first added and the solution pH was adjusted to approximately 4.4 with acetate buffer solution. The solution was sealed, mixed well, and left in the dark for 5 minutes. The color of the sample solution change to brownish yellow. The sample solution was then titrated using a 0.05 M standard $Na_2S_2O_3$ solution until the brownish yellow solution became pale yellow. 1.0 mL 1wt% starch solution was added as the indicator (the color of the sample solution became dark blue). Titration with the 0.05 M standard $Na_2S_2O_3$ solution was continued until the color disappeared. Finally, the amount of hypochlorite in the solution was calculated by recording the volume of the 0.05 M $Na_2S_2O_3$ solution used via equations S1-S3.

$$2\ KI + 2\ CH_3COOH \rightarrow 2\ CH_3COOK + 2\ HI \qquad (S1)$$

$$2 \text{ HI} + \text{NaClO} \rightarrow \text{NaCl} + \text{I}_2 + \text{H}_2\text{O} \qquad\qquad (S2)$$

$$\text{I}_2 + 2 \text{ NaS}_2\text{O}_3 \rightarrow 2\text{NaI} + \text{Na}_2\text{S}_4\text{O}_6 \qquad\qquad (S3)$$

All sample solution analysis was conducted by taking 2.0 mL electrolytes containing hypochlorite produced after electrolysis. The concentration of hypochlorite can be calculated with the volume of the $\text{Na}_2\text{S}_2\text{O}_3$ solution used in the titration process from the following equation S4.

$$C_{ClO^-}(M) = \frac{C_{Na_2S_2O_3} \times V_{Na_2S_2O_3}}{2 \times V_{ClO^-}} \qquad\qquad (S4)$$

where $C_{Na_2S_2O_3}(M)$, $V_{Na_2S_2O_3}(mL)$ and $V_{ClO^-}(mL)$ are the concentration of the $\text{Na}_2\text{S}_2\text{O}_3$ solution, the volume of the $\text{Na}_2\text{S}_2\text{O}_3$ solution used and the volume of the hypochlorite solution, respectively.

4. Detailed calculations of phase separation in the phase separator

Driving pressure, ΔP_{mem}, is given as the following:

$$\Delta P_{mem} = \rho g h \qquad\qquad (S6)$$

where ρ is the density of the retained phase, g is the acceleration of gravity, h is the height of the retained phase.

Drag pressure, P_{per}, can be approximated by the following:

$$P_{per} = \frac{8\mu Q L}{n\pi R^4} \qquad\qquad (S7)$$

where μ is the viscosity of the permeate phase, Q is the entering permeate liquid volumetric flow rate, L is the membrane thickness, n is the number of pores, and R is the pore radius.

Capillary pressure, P_{cap}, is a critical parameter which must be balanced with other forces in the device to guarantee proper operation of a separator. P_{cap} is given as the following:

$$P_{cap} = \frac{2\gamma\cos(\theta)}{r} \qquad\qquad (S8)$$

where γ is the interfacial tension between the two liquids to provide the force to achieve separation, θ is the contact angle between the solid material of the device and two liquid phases, and r is the radius of curvature of the interface.

Model values of permeate flow rate at different driving pressures were calculated by letting $P_{per} = \Delta P_{mem}$.

That is

$$\frac{8\mu QL}{n\pi R^4} = \Delta P_{mem} \tag{S9}$$

Therefore

$$Q = \frac{n\pi R^4}{8\mu L}\Delta P_{mem} \tag{S10}$$

For a certain membrane and hydrophobic phase, n, R, μ, L are constants, so Q is proportional to ΔP_{mem}, where was shown in Fig. S12.

5. Supporting Figures and Tables:
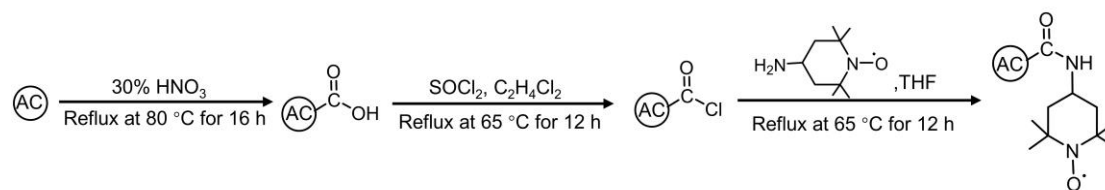
Fig. S1 The preparation route of TEMPO@AC[1].

Table S1 Textural characteristics and chemical composition of the materials.

Sample	S_{bet}(m²/g)	V_p(cm³/g)	Elemental analysis TEMPO (mmol /g)
Silica	633.7	0.97	-
TEMPO@Silica	412.7	0.54	0.304
COOH@AC	1085	0.55	-
TEMPO@AC	803.5	0.42	0.155
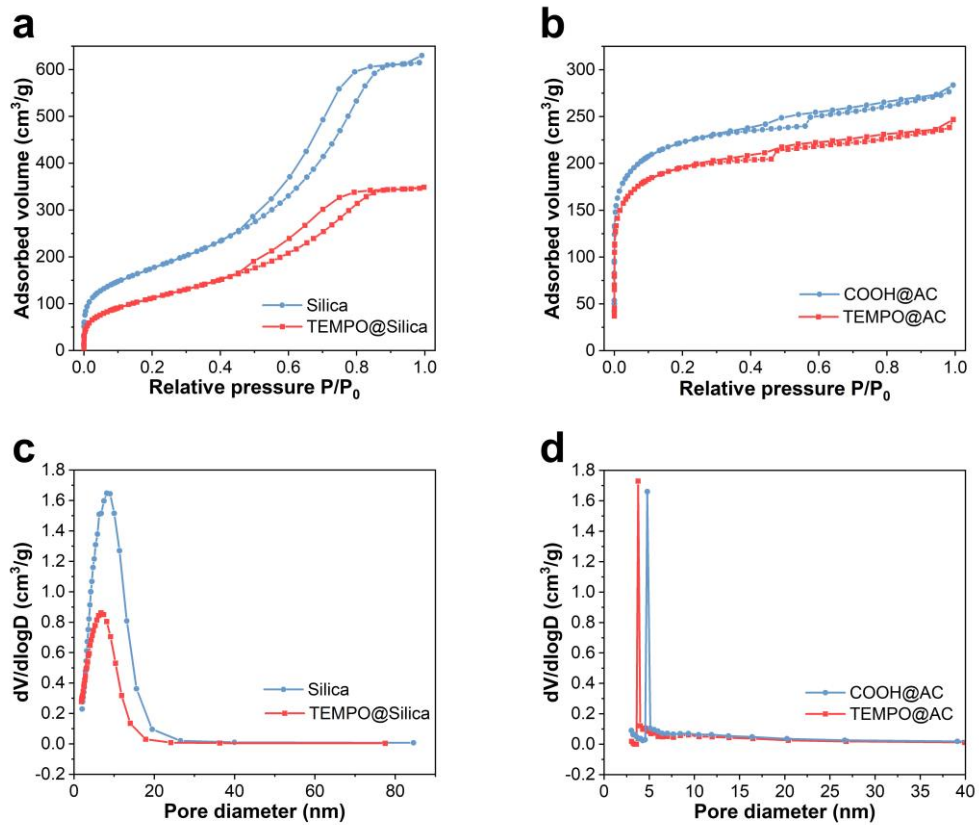
Fig. S2 (a)(b) N$_2$ adsorption/desorption plots, (c)(d) corresponding pore size distributions.
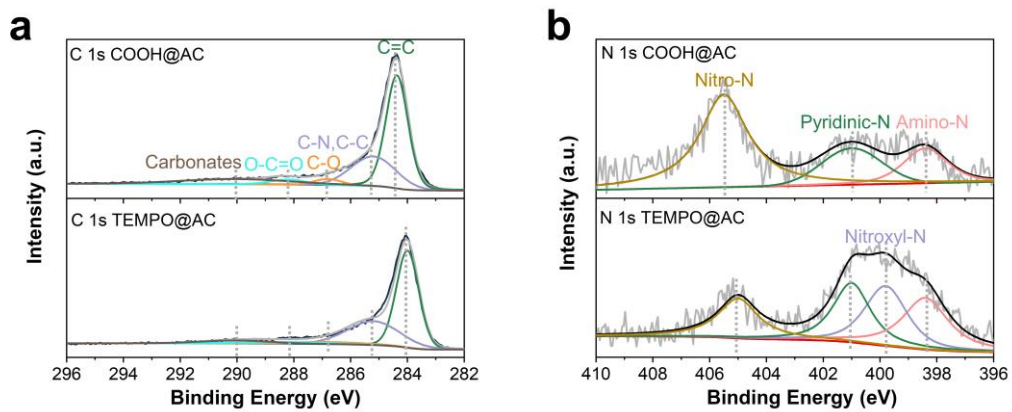
Fig. S3 (a) C 1s and (b) N 1s XPS spectra of COOH@AC and TEMPO@AC.
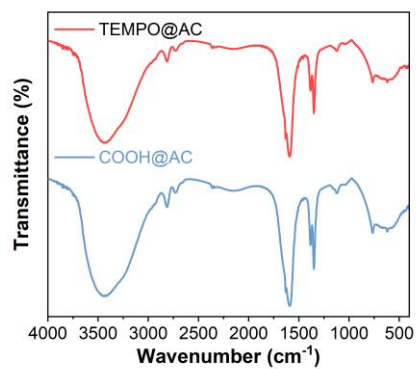
Fig. S4 IR spectra of COOH@AC and TEMPO@AC.
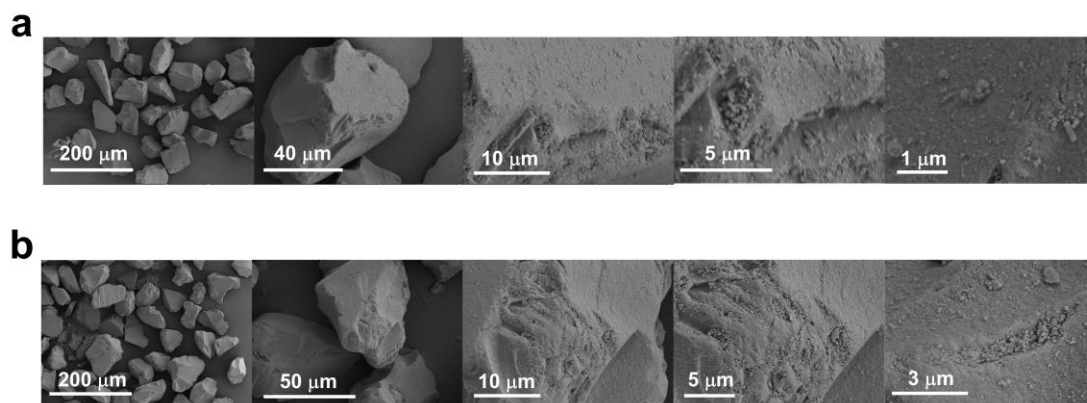
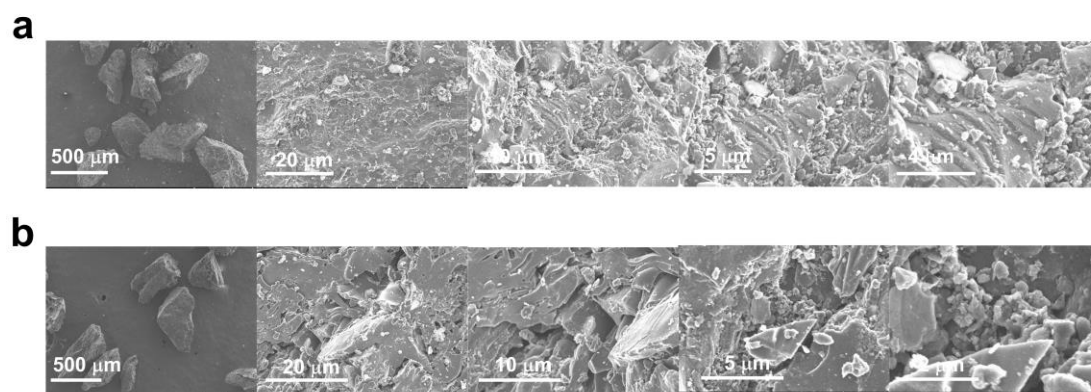**Fig. S5** SEM images for surface morphology of (a) Silica and (b) TEMPO@Silica.

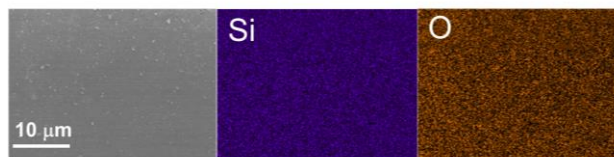**Fig. S6** SEM images for surface morphology of (a) COOH@AC and (b) TEMPO@AC.
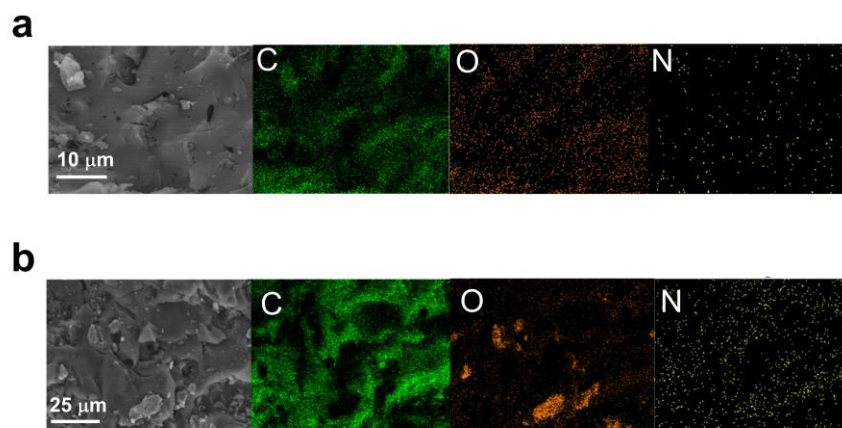
Fig. S7 Elemental mapping images of Silica.

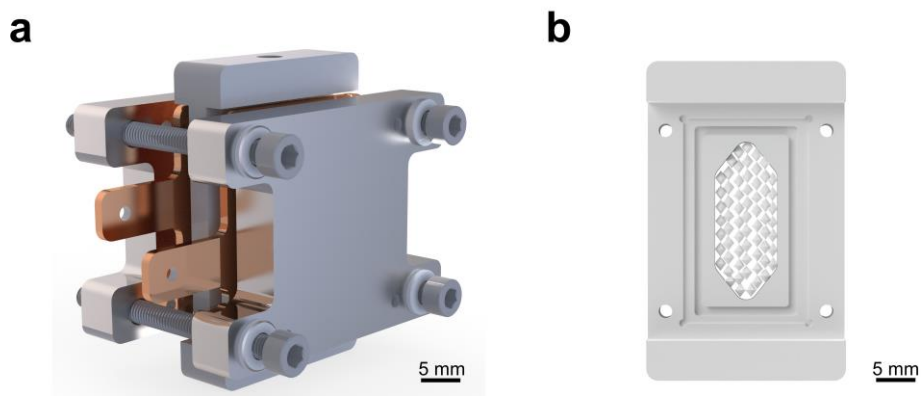**Fig. S8** Elemental mapping images of (a) COOH@AC and (b) TEMPO@AC.

Fig. S9 (a) A graph of configured electrochemical flow reactor. (b) Detailed graph of PTFE flow chamber filled with spiral static mixers.
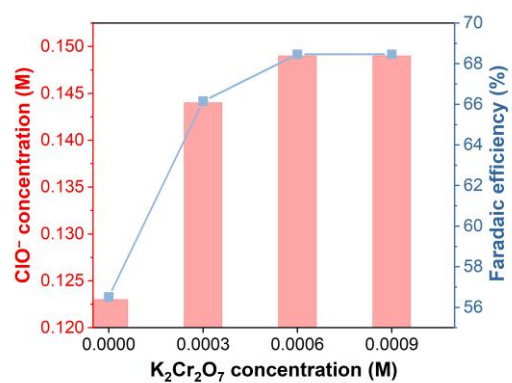
Fig. S10 Optimization of $K_2Cr_2O_7$ concentration in a batch electrolysis experiment. Reaction conditions: RuO_2/Ti (1×2 cm^2) anode, 304 stain-less steel (1×2 cm^2) cathode, 15 mL 3 M NaCl(aq), 700 mA, 350 mA/cm^2, 15 min, 1200 rpm.
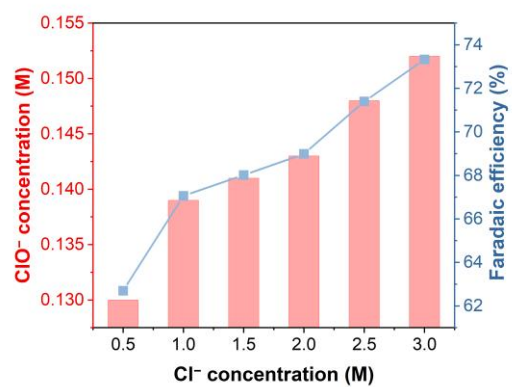
Fig. S11 Optimization of Cl⁻ concentration in a flow electrolysis experiment. Reaction conditions: NaCl(aq) (0.6 mM $K_2Cr_2O_7$), 168 mA/cm^2, 0.45 mL/ min electrolyte flow rate.
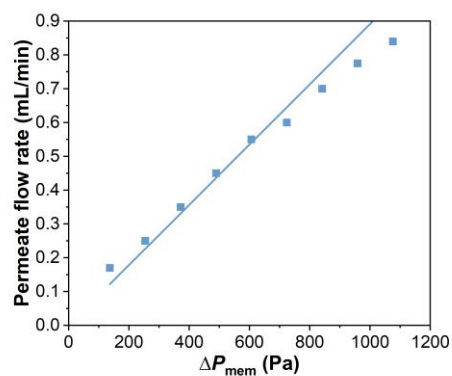
Fig. S12 Plot of model and experimental results of the PTFE hydrophobic membrane-based liquid-liquid phase separator (15 mm inner diameter, 13 cm high). Model values were given by the solid line while experimental values were given by squares. Testing conditions: Deionized water containing a small amount of $K_2Cr_2O_7$ as the color indicator was used as the testing retention phase, while DCM solvent was used as the testing permeate phase. DCM solvent was continuously pumped into the above space of the membrane at a certain water height (from 1.4 cm to 11 cm), and maximum permeate flow rate at a certain water height was determined by gradually increasing the pumped DCM flow rate until DCM still completely passed through the membrane.
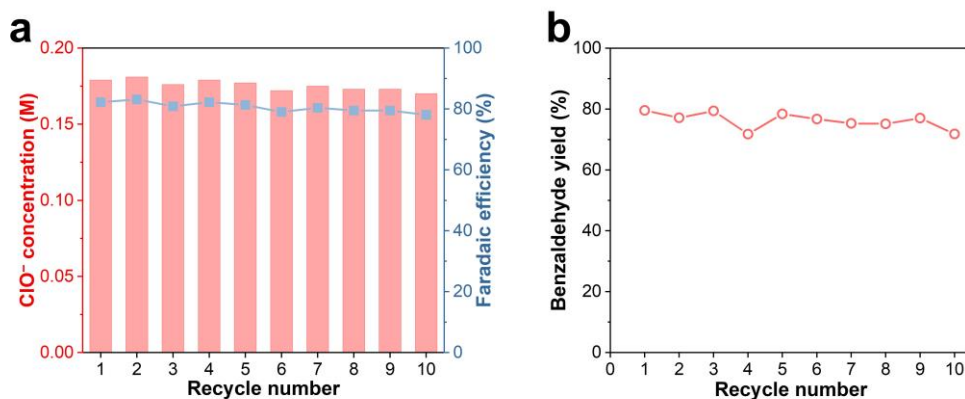
Fig. S13 The stability test of the recycled electrolytes in a batch recycling experiment. (a) Hypochlorite concentration and corresponding FE in ten recycle number. (b) Corresponding benzaldehyde yield in ten recycle number. Electrolysis conditions: RuO_2/Ti (1×2 cm^2) anode, stain-less steel (1×2 cm^2) cathode, 15 mL 3 M NaCl(aq) (0.6 mM $K_2Cr_2O_7$, 0.02 M NaBr); 700 mA, 350 mA/cm^2; room temperature; 800 rpm stirring; 15 min. Reaction conditions: 13 mL 0.2 M benzyl alcohol in DCM; 13 mL NaClO(aq) (~0.85 eq) collected by electrolysis of NaCl(aq); 1 mol% TEMPO@Silica catalyst; room temperature; 1000 rpm stirring.
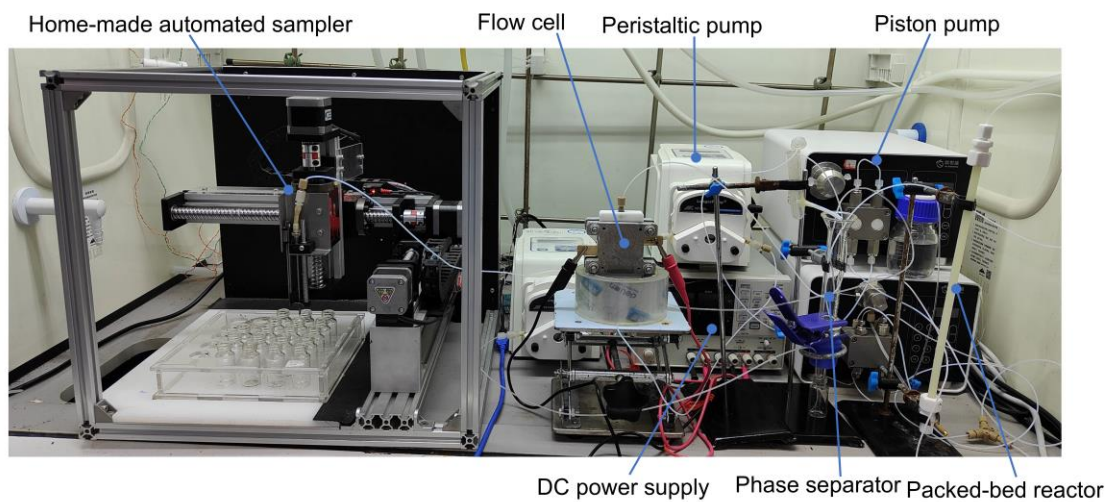
Fig. S14 A photograph of the closed-loop tandem electrochemical-chemical catalysis system.
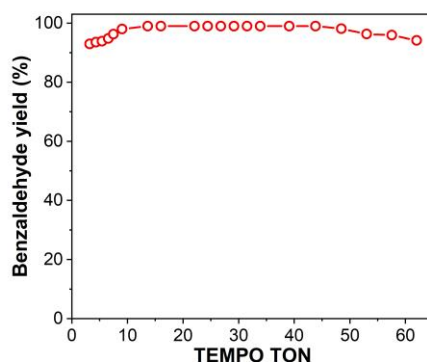
Fig. S15 The stability test of the closed-loop tandem electrochemical-chemical catalysis system using continuous oxidation of benzyl alcohol as a model reaction. Reaction conditions: A φ4 mm PTFE tube (18 cm long) filled with 1.67 g TEMPO@Silica (0.304 mmol/g); 0.2 M benzyl alcohol in DCM; 10 mL 1.5 M NaCl, 0.01 M NaBr, and 0.6 mM $K_2Cr_2O_7$ aqueous solution; room temperature; 168 mA/cm² and 0.45 mL/min electrolyte flow rate for electrochemical hypochlorite generation; 0.200 mL/min organic phase flow rate and 0.400 mL/min aqueous phase flow rate for TEMPO-catalyzed alcohol oxidation. The conversion and yield were characterized using GC with dodecane as the internal standard.

References

1 C. Zhang, M. Huang, J. Yin, F. Lou, X. Chen and J. Zhang, *Journal of Catalysis*, 2022, **413**, 968–977.